Optical Absorption Modeling of bilayer photoanode based on Cu@TiO2 Plasmonic Dye Sensitized Solar Cells towards Photovoltaic Applications

Zia Ur Rehman
Sarhad University of Science and Information Technology
Shahid Ali
Shanghai University
Muhammad Aslam
Hebei Normal University
Muhammad Idrees (m.idrees8223@gmail.com)
Shenzhen University
Anees Ur Rehman
Xi'an Jiaotong University
Javed Iqbal
Sarhad University of Science and Information Technology
Najeeb Ullah
University of Engineering and Technology
Said Karim Shah
Abdul Wali Khan University Mardan
Saima Batool
Shenzhen University

Research Article

Keywords: Dye-sensitized solar cell, Cu@TiO2, absorption efficiency, nanorods, short circuit current density

Posted Date: April 26th, 2021

DOI: https://doi.org/10.21203/rs.3.rs-452412/v1

Abstract

A periodic array of core–shell Cu@TiO_2 nanoparticle for plasmonic dye sensitized solar cells (DSSCs) in the wavelength range between 350–750 nm was studied. The size of copper nanospheres was 70 nm while the length and diameter of the copper nanorods were 100 and 10 nm, respectively. The UV-Visible absorption spectrum showed that the photo-anode based copper added TiO_2 has 29.3% absorption capability compared with copper-free TiO_2. TiO_2 with shell thickness of 5 nm coated copper exhibited the absorption efficiency of 71.9%, while short circuit current density of 17.52 mA cm^{-2} for Ci@TiO_2 photo-anode. This was attributed to a strong localized electric field around ultra-thin TiO_2-coated copper nanospheres. The UV-Visible results of different geometries indicated that the spherical-shaped Cu@TiO_2 nanoparticles induced the high absorption capability of 3.4% compared to rod-shaped Cu@TiO_2 nanoparticles. The hybrid nanorods/nanospheres bilayer photo-anode showed the high optical UV-Visible absorption of 11.42% as compared with nanospheres/nanorods, ascribed to the large surface area for dye-loading excellent light scattering.

1. Introduction

In dye-sensitized solar cells (DSSC), the conversion of photons into electric current begins with the absorption of light through sensitized dye molecules [1–4]. The excited sensitizer is oxidized by the injection of ultra-fast electrons into the conduction band of the semiconductor material [5–6]. Various optimization methods are reported to improve the photovoltaic performance of DSSC, including molecular designs to expand the absorption spectrum of dye and suppress the recombination rate [7–8], improving the electrolytic redox system [9–10], applying resistance engineering to reduce the internal impedance of the cell and increasing the light harvesting efficiency through scattering or plasmonic effect [11–14]. The localized surface plasmon resonance (LSPR) spectrum of metal nanoparticles contains both absorption and scattering components, which depends on the size, material composition, morphology of the nanoparticles and the dielectric medium surrounding the nanoparticles, thus needs to be finely tailored [15–17]. Moreover, the LSPR of metal nanoparticles is sensitized by the presence of another nearby nanoparticles, which can be considered as extreme interaction with the dielectric environment. When one nanoparticle is placed within a few nanometer range to other nanoparticle, the light-dependent dipole moment of the particles are coupled to each other, causing a sudden change in the absorption and scattering cross-sections of the nearby particles. Plasmonic coupling also causes a confined and strong electric field between the gaps of coupled nanoparticles [18]. This high restricted and improved electric field significantly improves the incompatibility between photons and molecules. LSPR can effectively convert electromagnetic energy into heat [19], thus can increase local temperature and induce nanoscale phase transitions. This thermal effect of LSPR has been widely used in thermotherapy, solar vapor production and photon induced drug release [20].

Metal nanoparticles have been used in the last decade to capture light in plasmonic dye sensitized solar cells [21–22]. The importance of gold and silver nanoparticles is due to their fascinating optical

properties. Several successful reports of incorporating metal nanoparticle directly in the active layer of DSSC have been published. However, the concern about corrosion of metal nanoparticles when they come in contact with dye and electrolyte molecules is still at its infant [23]. Moreover, these metal nanoparticles are oxidized by surrounding environment. To overcome these issues some reports proposed the idea of shielding of metal core with dielectric or polymeric shells [24, 25]. Recently, Hao et al. [26] demonstrated the addition of $Ag@SiO_2$ nanoparticles in the active layer of organic solar cell, which resulted in enhancement of power conversion efficiency by 19.2%. They linked this improvement to two key phenomena. First, the rise in extraction and transportation of holes and second, optical absorption by near-field enhancement and far-field scattering. Zohreh et al. [27] improved the performance of DSSC by adding copper to TiO_2. Their results showed that power conversion efficiency of CuO/TiO_2 nanocomposite is 43% higher than that of pure TiO_2. Ünlü et al. [28] synthesized different amount of copper doped TiO_2 and used as photo-anode materials in dye sensitized solar cell. The PCE of undoped TiO_2, 0.5% and 1% copper doped TiO_2 were recorded as 4.77%, 4.98% and 5.09% respectively. They observed that this enhancement is attributed to doping which can interact with dyes and caused change in charge transportation and recombination. However, up to best of our knowledge, their research is still insufficient as it lacks systematic studies on the effect of plasmon enhancement for various shell thicknesses and geometries of core-shell $Cu@TiO_2$ NPs. Since the optical intensity of the near field decreases quickly from the metal-dielectric boundary, LSPR should be optimized by changing the thickness of the shell to increase absorption efficiency. In order for the metal core to trap the incident light, the shell must provide optimal gap, good electrical conductivity, adequate chemical stability, as well as excellent photo-voltaic properties. As reported, TiO_2 as shell material would have two key benefits (i) energy band gap compatibility to dye sensitize and (ii) provide lowered internal impedance for the solar cell [29]. However, at the nanometer scale, the optical properties of TiO_2 can be significantly changed with varying shell thickness, there by affecting the plasmonic enhancement in DSSCs Therefore, the shell thickness and geometry of the nanoparticles need to be carefully designed to get optimal enhancement.

This study introduced core-shell $Cu@TiO_2$ as active photo-anode material to improve the optical absorption efficiency of DSSC devices. The incorporation of copper nanoparticle with two different spherical and rod shape morphology into photo-anode layer of DSSC and compare the effectiveness of nanoparticles morphology on the absorption capability of the device was introduced. Among the nanoparticle morphology studied, the highest optical absorption can be obtained by using the spherical-shaped copper nanoparticles coated with TiO_2. Considering the use of bilayer structures, the UV-VIS absorption of hybrid nanorods/nanosphere photo-anode is superior to nanospheres/nanorods, which are in accordance with obtained results [30]. The optical properties associated with these unique morphology and photo-anode structures will lead the copper nanoparticles for further development of solar cell technology.

2. Simulation Process

A typical core-shell Cu@TiO_2 based photo-anode structure of DSSC is schematically modeled. The computation was based on finite element method (FEM) that offers a standard 3-D discretization scheme, appropriate several high-frequency applications in frequency or time domain as reported in [31]. The basic idea of this numerical method is to apply the Maxwell's Equations in integral form which always mostly provide flexibility to the model. Here the absorption of photo anode is investigated from 35 to 750 nm wavelength range. Total absorption factor, A_{photon}, will estimate the optical absorption capability of model for different particle sizes arranged in different layers. A_{photon} is the ratio of absorbed photons by the model to the total incident photons in unit area.

2.1 Materials, geometry and boundary conditions

A model of photoactive layer of DSSC is created in this study as shown in Fig. 1. In our model, tetrahedral meshing is employed for frequency domain solver. Materials selected are defined by optical properties such as refractive index (n) and extinction coefficient (k) for which the data is selected from [32]. Silica glass was used for its advantages in both antireflection properties and surface passivation. The thickness of this layer is chosen as 40 nm. Plasmonic Ag NP is placed in the center of TiO_2 in each model. The size of copper nanoparticle is fixed to 70 nm, while shell thickness of TiO_2 was varying in the range between 5–20 nm. The diameter and length of the copper nanorods were 10 and 100 nm, respectively. Air is assumed as surrounding medium for the Cu@TiO_2 nanoparticle. Tetrahedral meshing of 10 nm size was employed for precise calculation. Periodic (p) array of nanoparticles was assumed to place on the top of fluorine doped tin oxide (FTO) with boundary condition along x and y directions. The size of period was taken as 20nm. A perfectly matched layer boundary conditions were used in the model to prevent stray reflections toward the nanoparticles. Incoming light is a plane wave that travels along the z direction and directions of magnetic and electric field are x and y respectively. The same DSSC model under same conditions without copper nanoparticles in the photoanode layer was also designed as reference to estimate the enhancement in absorption of Cu@TiO_2 based solar cell.

3. Results And Discussion

3.1 Localized surface plasmon resonance of core–shell Cu@TiO_2 nanospheres

In order to optimize the best suitable materials for photo-anode, we have studied the Tauc's curve of photo-anode based on TiO_2 coated copper nanospheres and copper-free TiO_2 nanospheres. It can be seen from Fig. 2 (a), the bandgap of bared TiO_2 (Cu-free TiO_2) and Cu@TiO_2 is 1.70 and 1.45 eV respectively. The reason of lower band gap is attributed to addition of copper nanospheres which increase the excitation rate of dye sensitizers by localized surface plasmon resonance [33]. A similar effect on the band gap was also reported by Babu et al [34]. Moreover, the metal cores can go through

charge equilibrium with the adjacent TiO_2 and alter its Fermi energy level, ensuing an enhanced cell potential.

The absorption enhancement of photo-anode based on $Cu@TiO_2$ is supported by the UV-VIS spectrum. UV-VIS spectrum of Cu-free TiO_2 and $Cu@TiO_2$ was compared in the range of 350–750 nm. As shown from Fig. 2 (b), the absorption capability of photo-anode based on Cu-free TiO_2 nanospheres and $Cu@TiO_2$ with 5 nm shell thickness is 55.6 and 71.9% respectively. The $Cu@TiO_2$ showed two significant absorption peaks at 510 and 695 nm while the Cu-free TiO_2 nanospheres showed the only peak at 540 nm. The absorption enhancement of photo-anode based on $Cu@TiO_2$ is 29.3% higher than that of copper-free TiO_2. This enhancement is attributed to the localized surface plasmon resonance excited by copper nanospheres which boosted up the optical performance of DSSC. Moreover, the addition of Cu metal core act as scattering centers for incident light and provides a longer path length for photons, resulting in improving their probability of being absorbed in the photo-anode layer, confirmed by the UV-VIS absorption curves (Fig. 2b).

3.2 Optimization of shell thickness

As the near-field effects are strongly distance dependent therefore the effect of shell thickness on the plasmon-based efficiency enhancement was investigated using $Cu@TiO_2$ nanoparticles with various shell thicknesses. The size of copper core is fixed at 70 nm, while the shell thickness (t) is varied from 5 to 20 nm. The comparative UV-VIS absorption spectrum of various shell thicknesses of $Cu@TiO_2$ and Cu-free TiO_2 is presented in Fig. 3 which clearly shows plasmonic resonance peaks around 510.5 and 695.5 nm with slight red shifts (3–10 nm). These red shifts of curves are attributed to dielectric behavior of copper nanospheres with changing shell thickness (t) from 5 to 20 nm. We have observed that optical absorption enhancement decrease with increasing the shell thickness (t). From Table 1, it can be seen that, enhancement of 20.1%, 23.5%, 25.8% and 29.3% is recorded for $Cu@TiO_2$ nanoparticles based photo-anode with shell thicknesses of 5, 10, 15 and 20 nm respectively compared to that of Cu-free TiO_2. This is because metal particles can act as optical antennas for incident light. When the copper nanospheres are placed near the TiO_2 Shell, LSPR produces strong near-field electromagnetic energy concentration which assists the direct injection of charge carriers from the plasmonic antenna into the conduction band of TiO_2 [35]

Table 1
Absorption enhancement and short circuit current density for different shell thickness of $Cu@TiO_2$ in comparison with Cu-free TiO_2.

Types of Photo-anode	Shell Thickness 't' (nm)	Absorption (%)	Absorption Enhancement (%)	Short Circuit Current Density ($mA\ cm^{-2}$)
Cu-free TiO_2	-	55.6	-	12.89
$Cu@TiO_2$	20	66.8	20.1	16.26
	15	68.7	23.5	16.79
	10	70	25.8	17.11
	5	71.9	29.3	17.52

Table 1 shows the enhancement in Jsc due to plasmonic Cu nanoparticles based photoanode. The Jsc increases from 12.89 mA/cm^2 to 17.52 mA/cm^2 after the incorporation of the plasmonic nanoparticles with shell thickness of 5nm. The Jsc improves by about 36% for the shell thickness of 5 nm while it only improves by 26.14% for the shell thickness of 20 nm. This shows that photovoltaic performance of plasmonic metal nanoparticles based solar cell is more enhanced than that of without plasmonic nanoparticle. The improvement of short circuit current density of solar cell using plasmonic nanoparticle is also reported in [36–38]. The Tauc's curves of Fig. 3(b) also supports the highest absorption enhancement of $Cu@TIO_2$ with Tsh = 5cm. Minute variation in the band gap energies is observed with varying shell thicknesses. These shifts are attributed to the dielectric properties of copper nanoparticles.

To gain insight on this phenomenon, we calculated the electric field intensity around metal nanospheres at the wavelength of λ = 510 nm. As it can be seen in Fig. 4 the electric field around the copper nanospheres is stronger for t = 5 nm. This reduced shell thickness encourages the near-field antenna effect associated with localized surface plasmon resonance and consequently enhances the absorption in the photo-anode layer.

3.3 Effect of $Cu@TiO_2$ nanoparticles geometry on absorption enhancement

In order to obtain the maximum improvement, it is necessary to understand the effect of particle morphology on the absorption performance of DSSC. In this study, we were able to provide good optical performance by comparing the spherical- and rod-shaped structures of nanoparticles which are confirmed by the broadband UV-VIS absorption analysis of Fig. 5. Based on results of Sect. 3.2, we have considered the results of spherical geometry of copper-free and copper incorporated TiO_2 nanoparticles with shell thickness of 5 nm for their best performance. By changing the morphology of copper

nanoparticles in the form of nanorods (NR), the UV-VIS absorption results showed 69.54% absorption capacity. The absorption capacity of the photo-anode based on rod-shaped Cu@TiO_2 nanoparticles is 25% higher than that of rod-shaped TiO_2 copper-free. It was observed that core-shell rod-shaped Cu@TiO_2 nanoparticles have a wider LSPR band with a peak at 420 nm. This absorption was owing to the high localized electric field strength of the Cu@ TiO_2 nanoparticles. The nanorods structure of Cu@TiO_2 nanoparticles captured the incident light, which resulted in increased path length of the incident light. This higher path depth length greatly improves the interaction between the dye molecules and the photons, resulting in producing more charge carriers [39–40]. However, the absorption enhancement of spherical-shaped Cu@TiO_2 is little higher (3.45%) than that of rod-shaped nanoparticles. It may be due to the fact that the spherical-shaped Cu@TiO_2 provides large surface area for dye absorption. This increased light diffusion capacity resulted in more electrons injection into the Cu@TiO_2 conduction band [41]. Moreover, the improvement occurs in the longer wavelength, which is the most desirable wavelength range required for the light absorption efficiency in the DSSC. Nevertheless, the rod-shaped Cu@TiO_2 photo-anode has also very important effect on DSSC performance. Tauc's curve of Fig. 5(b), it can be seen that the bandgap energies for spherical- and rod-shaped geometries of Cu embedded TiO_2 were 1.3 and 1.45 eV respectively. The reason for the reduced bandgap energy for spherical-shaped Cu@TiO2 is attributed to the large amount of dye molecules due to the large surface area provided by the spherical-shaped particles. According to the Beer–Lambert law, higher absorbance in the UV–vis spectrum means higher dye concentration.

3.4 Bilayer hybrid structure of Cu@TiO_2 nanorods and nanospheres

Nanostructured bilayer photo-anode has been modeled for high optical absorption photoanode by modifying with nanospheres (NS) and nanorods (NR). As discussed in Sect. 3.3, the modification of Cu@TiO_2 morphology in the form of nanorods causes the coming light to trap and increases the path depth length of light. This can substantially increase the photon interaction with the dye molecules and resulted in boosting the performance of photoanode. The spherical-shaped morphology of Cu@TiO_2, on the other hand, will provide adequate surface area which produces many excited electrons that are injected into the conduction band of Cu@TiO_2 and led to effective charge transportation. Comparing with the different photo-anode structures [42, 43], the novel hybrid photoanode in this study is capable to offer good optical performance as confirmed by broad band UV-VIS absorption spectrum (Fig. 7). The model for Cu@TiO_2 nanorods over Cu@TiO_2 nanospheres (NR/NS) bilayer and Cu@TiO_2 nanospheres over Cu@TiO_2 nanorods (NS/NR) structures are shown in Fig. 6. The UV-VIS absorption spectrum showed that the overall improvement in absorption of photo-anode based on NR/NS and NS/NR is 78.33 and 70.30% respectively. So, the NR/NS Cu@TiO_2 layer has 11.42% higher absorption compared to NS/NR because of following reasons (1) the upper NR layer exhibits higher light-scattering ability; and (2) the bottom Cu@TiO_2 nanospheres layer offers large surface area for dye absorption and thus provide more electrons in the conduction band of electrode. The enhancement takes place in the higher wavelength side, which is

more suitable wavelength range for light absorption efficiency in DSSCs [44]. However, the role of NS/NR Cu@TiO_2 photo-anode has also very important influence on the performance of DSSCs.

The Tauc's curve of Fig. 7(b) shows that the bandgap energies of photoanode's based on nanorods/nanospheres and nanospheres/nanorods are 1.4 and 1.51 eV, respectively. The reason for the reduced bandgap energy of the nanorods/nanospheres photoanode is attributed to the scattering effect of large-sized particles in the top layer of the rod-shaped nanoparticles. The light scattered by the top layer triggered an enhancement in the optical absorption. Thus, the combination of localized surface-plasmon resonance and the narrow bandgap of the bilayer structure led to the photoanode's enhanced light harvesting efficiency.

3.5 Normalized absorption and short circuit current density values of different photo-anode structures

- From Table 2, it is evident that all structures of photo-anode based on copper incorporated TiO_2 have higher absorption than that pure TiO_2. The enhancement in absorption attributed to addition of copper which exhibits localized surface plasmon resonance effect. Moreover, the bilayer photo anode structures have higher absorption capability than single layer structures (nanospheres and nanorods) which is endorsed to higher optical depth length of bilayer structure. The light confined for more time which gave rise further dye interaction with photons and resulted in higher absorption efficiency and short circuit current density.

The photoanode layers do not produce free carriers directly on photo excitation, instead producing a bound electron-hole pair (exciton). This exciton is separated to form free carriers at the electron-donor and electron-acceptor interface of the photovoltaic device. The effective generation of free carriers upon photoexcitation is therefore dependent on the retention of the exciton as it successfully creates free carriers. This is determined by the lifetime and diffusion length of the exciton. Free charges are easily created from the excitons generated close to the p-n interface. Increasing the interface area for dye absorption boosts the charge generation. It is the reason that the short circuit current density of photoanode based on nanospheres is 4.03% higher than that of nanorods. The generation of more charges due to more surface area resulted in efficient charge transport. Similar is the case of photoanode based bilayer nanosphere and nanorod. The nanorod/nanosphere (NR/NS) provides more area for dye absorption compared to that of nanosphere/nanorod therefore an increment of 11.4 % is observed in higher short circuit current density of NR/NS than NS/NR.

Table 2
Absorption enhancement and short circuit current density for different photo-anode structures based on $Cu@TiO_2$ in comparison with Cu-free TiO_2.

Types of $Cu@TiO_2$ photo-anode structures	Absorption (%)	Absorption enhancement w.r.t Cu-free based photoanode (%)	Short circuit current density ($mA\ cm^{-2}$)
Nanospheres	71.9	29.3	17.52
Nanorods	69.54	25.12	16.84
Bilayer nanosphere/nanorod	70.30	26.43	16.91
Bilayer nanorod/nanosphere	78.33	40.88	18.84

Conclusions

In this study, we have systematically studied the different morphology of copper as plasmon nanoparticles in photo-anode to enhance the absorption efficiency of DSSCs. The UV-Visible absorption spectrum showed that the photo-anode based on copper added TiO_2 nanospheres has 29.3% higher absorption capability than that of copper-free TiO_2. This enhancement is attributed to the strong electric field localization originated around plasmonic core–shell copper nanospheres. The optical response and short circuit current density of $Cu@TiO_2$ nanospheres were also studied with varying shell thickness. It was found that $Cu@TiO_2$ nanospheres with 5 nm shell thickness exhibited the highest absorption efficiency and enhanced short current density of 71.90% and 17.52 $mA\ cm^{-2}$ respectively. This enhancement is credited to strong surface plasmon resonance effect which is higher for small shell thickness [44]. Addition of Copper nanoparticles with both the spherical- and rod-shaped geometries resulted in improvement in the performances of DSSC. The photo-anode based on spherical-shaped $Cu@TiO_2$ nanoparticles has 29.3% higher absorption than that of the Cu-free TiO_2. Similarly, the absorption enhancement of the rod-shaped $Cu@TiO_2$ nanoparticles was 25% higher as compared to Cu-free TiO_2. The enhancement of spherical- and rod-shaped $Cu@TiO_2$ photo-anode was attributed to large surface area for dye-loading as well as excellent light scattering enhancement capacity. Bi-layered $Cu@TiO_2$ photo-anode consisting of nanospheres/nanorods and nanorods/nanospheres was also investigated for DSSCs. The bilayer nanorods/nanospheres $Cu@TiO_2$ exhibited 11.42% improved optical absorption as compared to the photo-anode based on nanospheres/nanorods $Cu@TiO_2$.

Declarations

Conflicts of interest

There are no conflicts to declare.

Acknowledgement

This research did not receive any specific grant from funding agencies in the public, commercial, or not-for-profit sectors. However, the Board of Advanced Studies and Research (BASR), Sarhad University of Science and Technology (SUIT), Peshawar, Pakistan provided the open

research platform and research facilities for this project.

References

[1] Rehman, A.U., Aslam, M., Shahid, I., Idrees, M., Khan, A.D., Batool, S. and Khan M., 2020. Enhancing the light absorption in dye-sensitized solar cell by using bilayer composite materials based photo-anode. Optics Communications, 126353.

[2] Hosseinnezhad, M., 2019. Enhanced performance of dye-sensitized solar cells using perovskite/DSSCs tandem design. Journal of Electronic Materials, 9, 5403-5408.

[3] Liu, Q., Sun, Y., Yao, M., Xu, B., Liu, G., Hussain, M.B., Jiang, K. and Li, C., 2019. Au@Ag@ Ag2S heterogeneous plasmonic nanorods for enhanced dye-sensitized solar cell performance. Solar Energy, 185, 290-297.

[4] Rehman, A.U., Aslam, F. and Khan, H.A., 2014. Analyze the Absorption Properties and IV Characterization of Dye Sensitized Solar Cell Using Ruthenium Dye, American Journal of Engineering and Applied Sciences, 4, 387-390.

[5] Fan, W.J., Chang, Y.Z., Zhao, J.L., Xu, Z.N., Tan, D.Z. and Chen, Y.G., 2018. A theoretical study of fused thiophene modified anthracene-based organic dyes for dye-sensitized solar cell applications. New Journal of Chemistry, 24, 20163-20170.

[6] Yang, Z., Shao, D., Li, J., Tang, L. and Shao, C., 2018. Design of butterfly type organic dye sensitizers with double electron donors: The first principle study. Spectrochimica Acta Part A: Molecular and Biomolecular Spectroscopy, 196, 385-391.

[7] Li, P., Song, C., Wang, Z., Li, J. and Zhang, H., 2018. Molecular design towards suppressing electron recombination and enhancing the light-absorbing ability of dyes for use in sensitized solar cells: a theoretical investigation. New Journal of Chemistry, 15, 12891-12899.

[8] Li, X., Zhang, X., Hua, J. and Tian, H., 2017. Molecular engineering of organic sensitizers with o, p-dialkoxyphenyl-based bulky donors for highly efficient dye-sensitized solar cells. Molecular Systems Design & Engineering, 2, 98-122.

[9] Hao, Y., Yang, W., Zhang, L., Jiang, R., Mijangos, E., Saygili, Y., Hammarström, L., Hagfeldt, A. and Boschloo, G., 2016. A small electron donor in cobalt complex electrolyte significantly improves efficiency in dye-sensitized solar cells. Nature Communications, 1, 1-8.

[10] Gao, J., Yang, W., El-Zohry, A.M., Prajapati, G.K., Fang, Y., Dai, J., Hao, Y., Leandri, V., Svensson, P.H., Furó, I. and Boschloo, G., 2019. Light-induced electrolyte improvement in cobalt tris (bipyridine)-mediated dye-sensitized solar cells. Journal of Materials Chemistry A, 33, 19495-19505.

[11] Sarker, S., Seo, H.W., Seo, D.W. and Kim, D.M., 2017. Electrochemical impedance spectroscopy of dye-sensitized solar cells with different electrode geometry. Journal of Industrial and Engineering Chemistry, 45, 56-60.

[12] Ullah, H., Khan, A.D., Noman, M. and Rehman, A.U., 2018. Novel multi-broadband plasmonic absorber based on a metal-dielectric-metal square ring array. Plasmonics, 2, 591-597.

[13] Ghadari, R., Sabri, A., Saei, P.S., Kong, F.T. and Marques, H.M., 2020. Phthalocyanine-silver nanoparticle structures for plasmon-enhanced dye-sensitized solar cells. Solar Energy, 198, 283-294.

[14] Kaur, N., Mahajan, A., Bhullar, V., Singh, D.P., Saxena, V., Debnath, A.K., Aswal, D.K., Devi, D., Singh, F. and Chopra, S., 2020. Ag ion implanted TiO2 photoanodes for fabrication of highly efficient and economical plasmonic Dye Sensitized Solar Cells. Chemical Physics Letters, 740, 137070.

[15] Sui, M., Kunwar, S., Pandey, P. and Lee, J., 2019. Strongly confined localized surface plasmon resonance (LSPR) bands of Pt, AgPt, AgAuPt nanoparticles. Scientific Reports, 1, 1-14.

[16] Khan, I., Saeed, K. and Khan, I., 2019. Nanoparticles: Properties, applications and toxicities. Arabian Journal of Chemistry, 7, 908-931.

[17] Pandey, Puran, Sundar Kunwar, and Jihoon Lee. 2020. Solid state dewetting of Ag/Pt bilayers for the stronger localized surface plasmon resonance (LSPR) properties: The dynamic control of surface morphology and elemental composition of AgPt and Pt nanostructures by the auxiliary Ag layer, Journal of Alloys and Compounds, 813, 152193.

[18] Khurgin, J., Tsai, W.Y., Tsai, D.P. and Sun, G., 2017. Landau damping and limit to field confinement and enhancement in plasmonic dimers. ACS Photonics, 11, 2871-2880.

[19] Ren, Y., Qi, H., Chen, Q., Wang, S. and Ruan, L., 2017. Localized surface plasmon resonance of nanotriangle dimers at different relative positions. Journal of Quantitative Spectroscopy and Radiative Transfer, 199, 45-51.

[20] Li, J., Liu, J. and Chen, C., 2017. Remote control and modulation of cellular events by plasmonic gold nanoparticles: implications and opportunities for biomedical applications. ACS Nano, 3, 2403-2409.

[21] Bao, Z., Fu, N., Qin, Y., Lv, J., Wang, Y., He, J., Hou, Y., Jiao, C., Chen, D., Wu, Y. and Dai, J., 2019. Broadband Plasmonic Enhancement of High-Efficiency Dye-Sensitized Solar Cells by Incorporating Au@Ag@SiO2 Core–Shell Nanocuboids. ACS Applied Materials & Interfaces, 1, 538-545.

[22] Rai, P., 2019. Plasmonic noble metal@metal oxide core–shell nanoparticles for dye-sensitized solar cell applications. Sustainable Energy & Fuels, 1, 63-91.

[23] Kaur, N., Mahajan, A., Bhullar, V., Singh, D.P., Saxena, V., Debnath, A.K., Aswal, D.K., Devi, D., Singh, F. and Chopra, S., 2019. Fabrication of plasmonic dye-sensitized solar cells using ion-implanted photoanodes. RSC Advances, 35, 20375-20384.

[24] Salimi, K., Atilgan, A., Aydin, M.Y., Yildirim, H., Celebi, N. and Yildiz, A., 2019. Plasmonic mesoporous core-shell Ag-Au@TiO2 photoanodes for efficient light harvesting in dye sensitized solar cells. Solar Energy, 193, 820-827.

[25] Kumar, P., Narayan Maiti, U., Sikdar, A., Kumar Das, T., Kumar, A. and Sudarsan, V., 2019. Recent advances in polymer and polymer composites for electromagnetic interference shielding: review and future prospects. Polymer Reviews, 4, 687-738.

[26] Hao, Y., Song, J., Yang, F., Hao, Y., Sun, Q., Guo, J., Cui, Y., Wang, H. and Zhu, F., 2015. Improved performance of organic solar cells by incorporating silica-coated silver nanoparticles in the buffer layer. Journal of Materials Chemistry C, 5, 1082-1090.

[27] Ünlü, B. and Özacar, M., 2020. Effect of Cu and Mn amounts doped to TiO2 on the performance of DSSCs. Solar Energy, 196, 448-456.

[28] Mahmoudabadi, Z.D. and Eslami, E., 2019. One-step synthesis of CuO/TiO2 nanocomposite by atmospheric microplasma electrochemistry–Its application as photoanode in dye-sensitized solar cell. Journal of Alloys and Compounds, 793, 336-342.

[29] Zhao, A., An, J., Yang, J. and Yang, E.H., 2018. Microencapsulated phase change materials with composite titania-polyurea (TiO2-PUA) shell. Applied Energy, 215, 468-478.

[30] Wang, D., Zhang, Y., Su, M., Xu, T., Yang, H., Bi, S., Zhang, X., Fang, Y. and Zhao, J., 2019. Design of Morphology-Controllable ZnO Nanorods/Nanoparticles Composite for Enhanced Performance of Dye-Sensitized Solar Cells. Nanomaterials, 7, 931-940.

[31] Chandrasekhar, P.S., Parashar, P.K., Swami, S.K., Dutta, V. and Komarala, V.K., 2018. Enhancement of Y123 dye-sensitized solar cell performance using plasmonic gold nanorods. Physical Chemistry Chemical Physics, 14, 9651-9658.

[32] Ni, X., Liu, Z. and Kildishev, A.V., 2007. PhotonicsDB: optical constants. https://nanohub.org/resources/PhotonicsDB

[33] Aneesiya, K.R. and Louis, C., 2020. Localized surface plasmon resonance of Cu-doped ZnO nanostructures and the material's integration in dye sensitized solar cells (DSSCs) enabling high open-circuit potentials. Journal of Alloys and Compounds, 154497.

[34] Babu, S.G., Vinoth, R., Kumar, D.P., Shankar, M.V., Chou, H.L., Vinodgopal, K. and Neppolian, B., 2015. Influence of electron storing, transferring and shuttling assets of reduced graphene oxide at the interfacial copper doped TiO2 p–n heterojunction for increased hydrogen production. Nanoscale, 17, 7849-7857.

[35] Ma, J. and Gao, S., 2019. Plasmon-Induced Electron–Hole Separation at the Ag/TiO2 (110) Interface. ACS Nano, 12, 13658-13667.

[36] Choudhury, S.A., Nawshin, N. and Chowdhury, M.H., 2017, November. Influence of particle shape on the efficacy of plasmonic metal nanoparticles to enhance the energy conversion efficiency of thin-film solar cells. In TENCON 2017-2017 IEEE Region 10 Conference IEEE. 2393-2398.

[37] Deng, W., Yuan, Z., Liu, S., Yang, Z., Li, J., Wang, E., Wang, X. and Li, J., 2019. Plasmonic enhancement for high-efficiency planar heterojunction perovskite solar cells. Journal of Power Sources, 432,112-118.

[38] Ali, Z., Amin, W., Khan, A.D., Khan, A.D., Imran, M. and Noman, M., 2021. Improving the light absorption efficiency in thin-film plasmonic tandem solar cell. Journal of Optics, 1-8.

[39] Dou, Y., Wu, F., Mao, C., Fang, L., Guo, S. and Zhou, M., 2015. Enhanced photovoltaic performance of ZnO nanorod-based dye-sensitized solar cells by using Ga doped ZnO seed layer. Journal of Alloys and Compounds, 633, 408-414.

[40] Ganesh, R.S., Navaneethan, M., Ponnusamy, S., Muthamizhchelvan, C., Kawasaki, S., Shimura, Y. and Hayakawa, Y., 2018. Enhanced photon collection of high surface area carbonate-doped mesoporous TiO2 nanospheres in dye sensitized solar cells. Materials Research Bulletin, 101, 353-362.

[41] Chandrasekhar, P.S., Parashar, P.K., Swami, S.K., Dutta, V. and Komarala, V.K., 2018. Enhancement of Y123 dye-sensitized solar cell performance using plasmonic gold nanorods. Physical Chemistry Chemical Physics, 14, 9651-9658.

[42] Liu, Q., Wei, Y., Shahid, M.Z., Yao, M., Xu, B., Liu, G., Jiang, K. and Li, C., 2018. Spectrum-enhanced Au@ZnO plasmonic nanoparticles for boosting dye-sensitized solar cell performance. Journal of Power Sources, 380, 142-148.

[43] Guli, M., Bimenyimana, T., Deng, M., Chen, S. and Long, J., 2018. Enhanced photoelectric performance of nanorod TiO2 film embedded with gold nanoparticles applied in dye sensitized solar cells studied by OptiFDTD. Optical Materials, 83, 200-206.

[44] Saliminasab, M., Garaei, M.A., Moradian, R. and Nadgaran, H., 2018. Novel and Sensitive Core-Shell Nanoparticles Based on Surface Plasmon Resonance. Plasmonics, 1, 155-161.

Figures

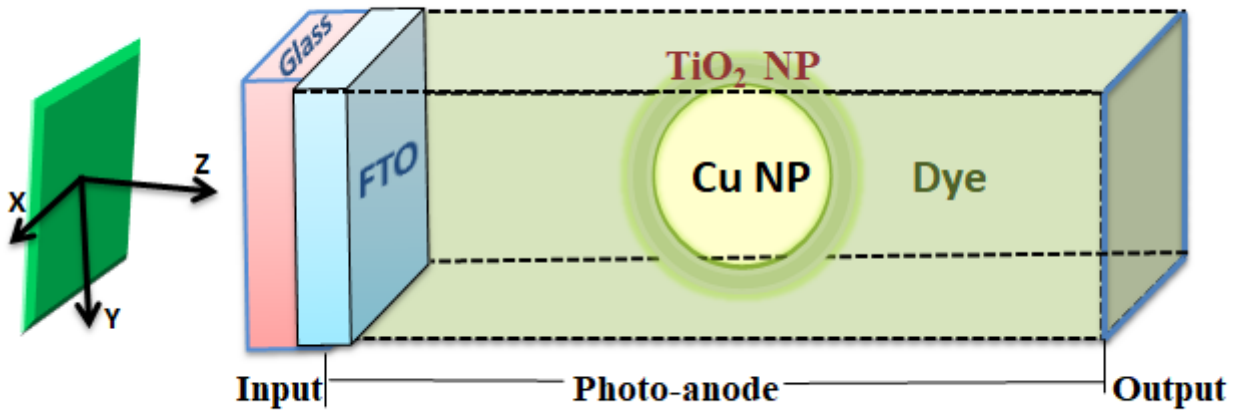

Figure 1

Model of photo-anode layer of DSSC with core-shell Cu@TiO2 nanoparticle

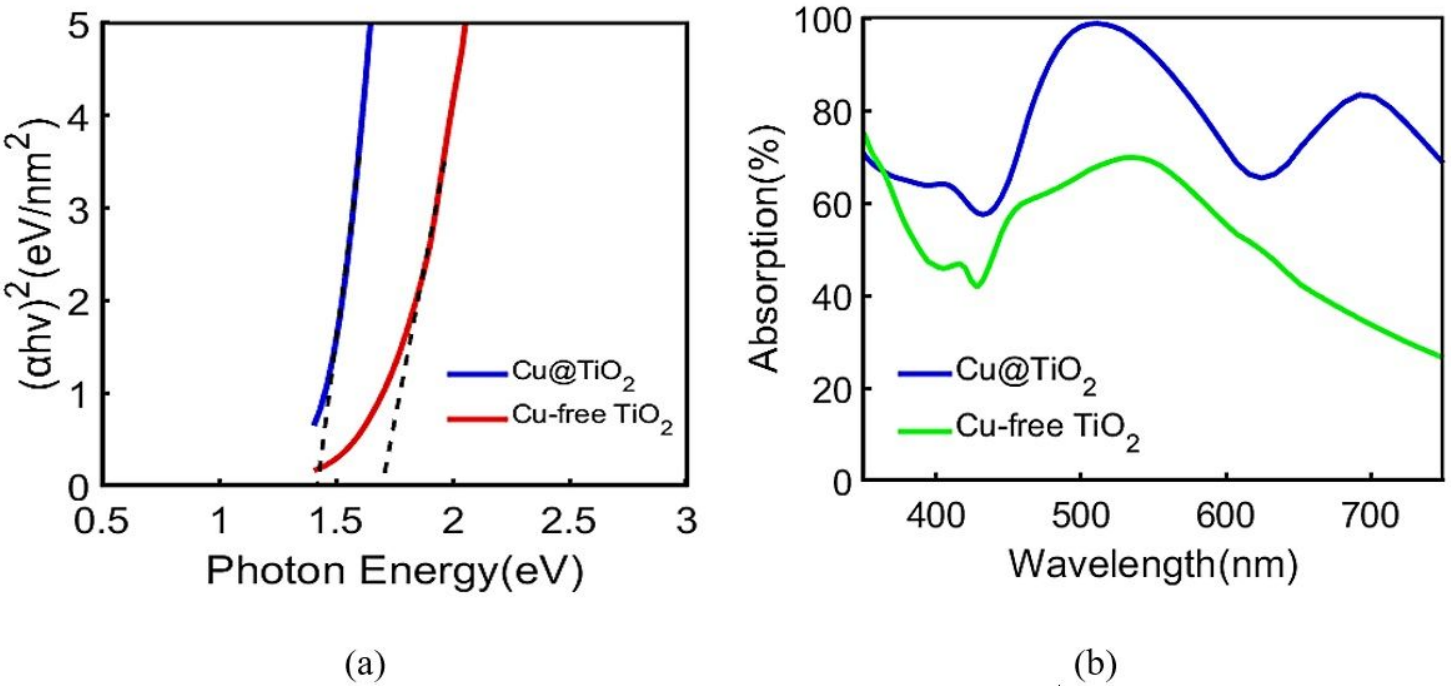

Figure 2

Results of Photo-anode based on Cu-free TiO2 and Cu@TiO2 nanospheres with 5 nm shell thickness (a) Tauc's curve (b) UV-VIS absorption

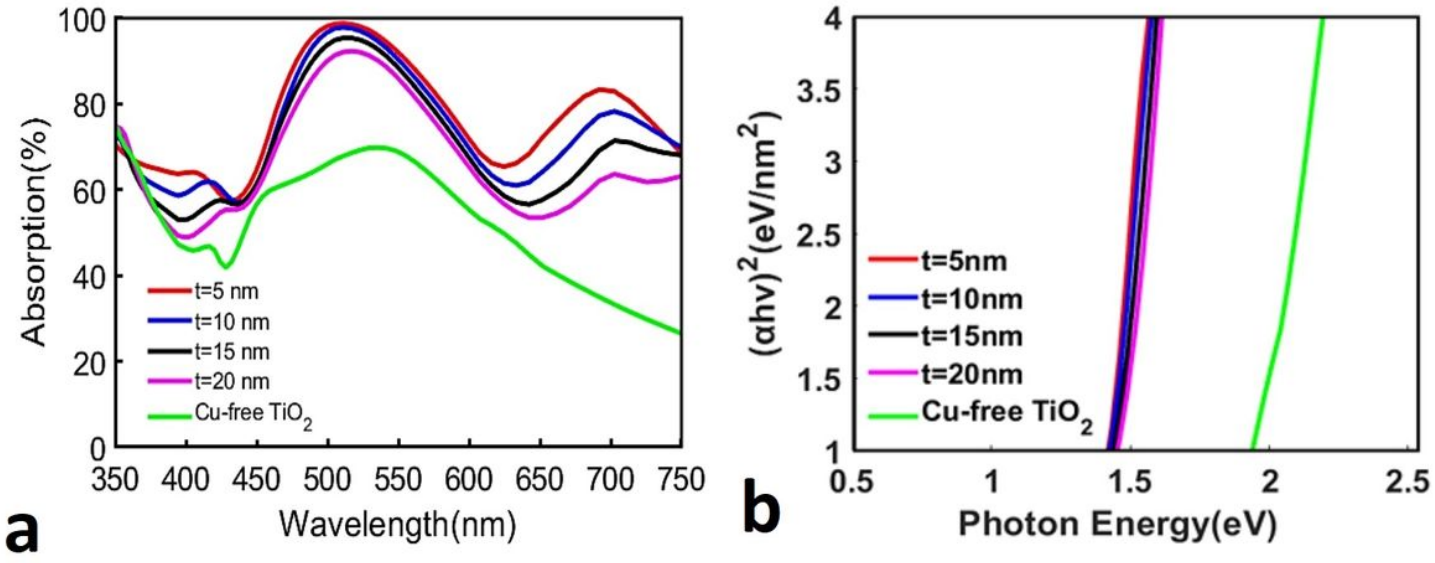

Figure 3

Results for photo-anode based on Cu-free TiO2 and Cu@TiO2 nanospheres with different thickness of the shell (a) UV-VIS absorption spectrum (b) Tauc's curves

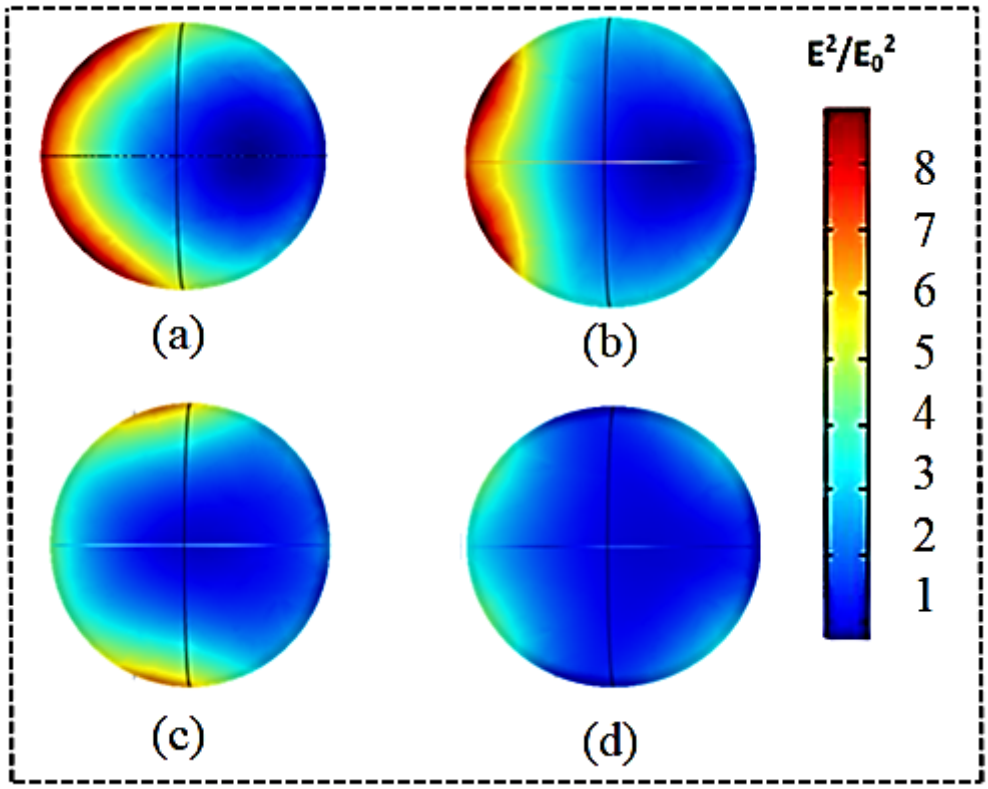

Figure 4

Electric field intensity distribution of Cu@TiO2 at 510 nm for shell thickness of (a) 5 (b) 10 (c) 15 and (d) 20 nm

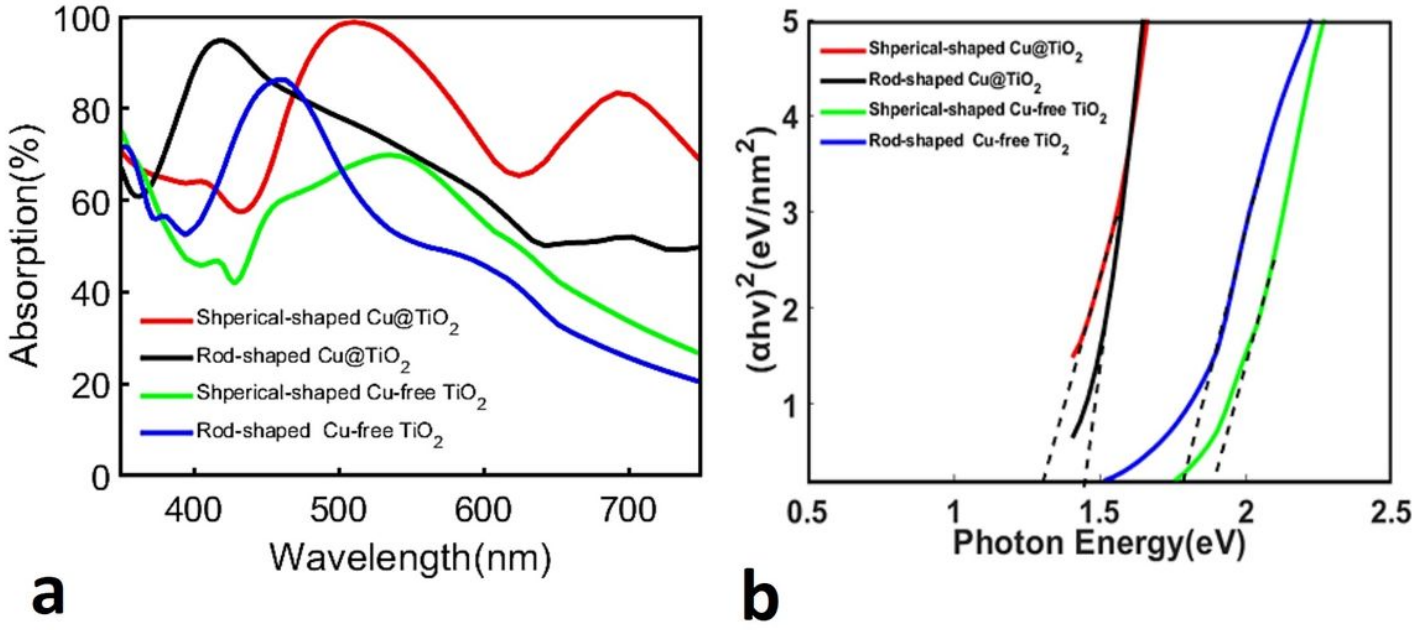

Figure 5

Results for photo-anode based on spherical- and rod-shaped geometries of Cu-free TiO2 and Cu@TiO2 (a) UV-Vis absorption cuves (b) Tauc's curves

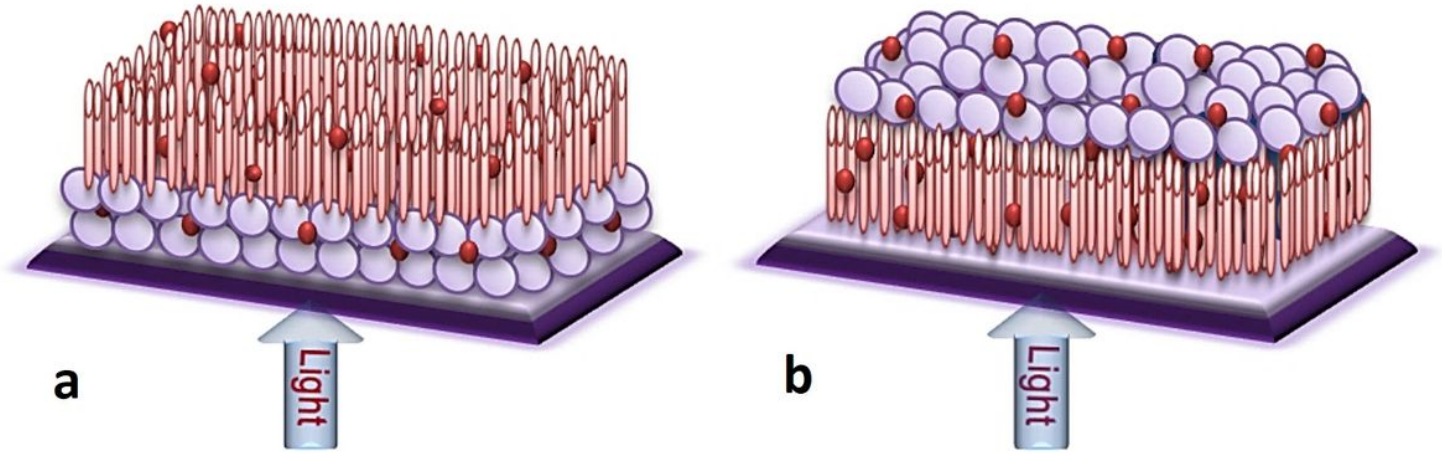

Figure 6

Schematic presentation of the Cu@TiO2 photo-anode based on (a) nanorods/ nanospheres (NR/NS) and (b) nanospheres/nanorods (NS/NR)

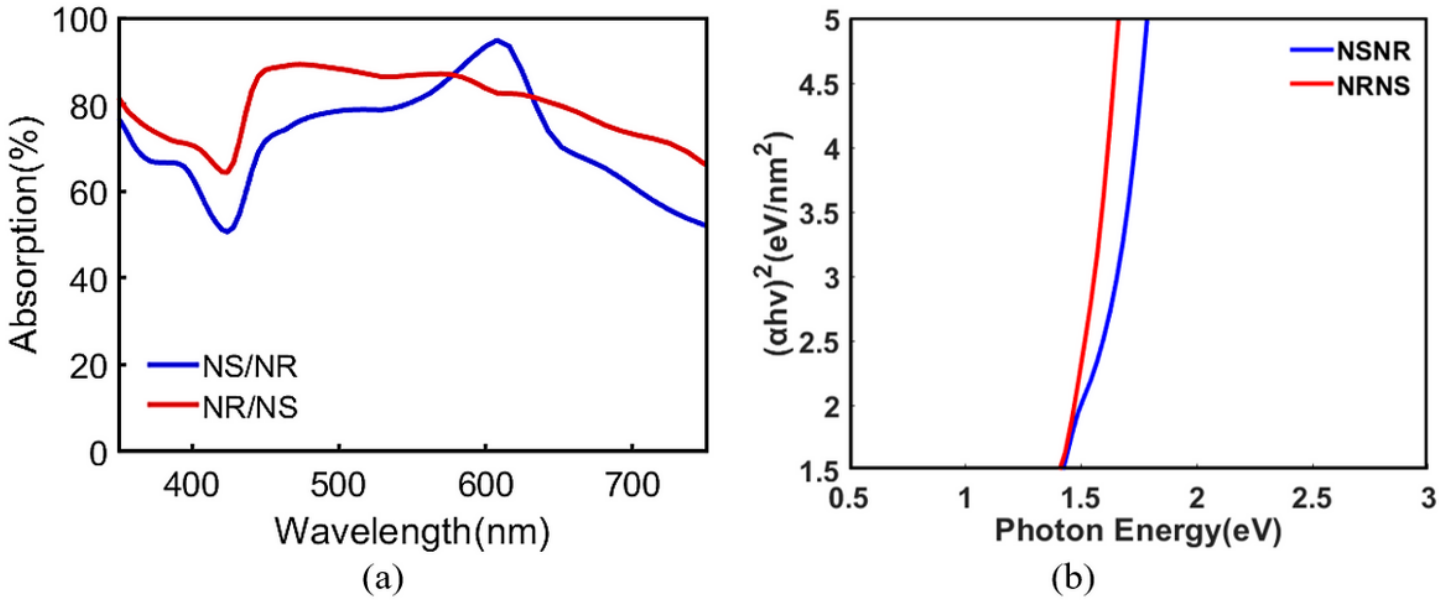

Figure 7

Bilayer Cu@TiO2 photo-anode based on nanorods/ nanospheres (NR/NS) and nanospheres/nanorods (NS/NR) (a) UV-VIS absorption (b) Tauc's curve